RSC Advances

PAPER

View Article Online
View Journal | View Issue

Cite this: *RSC Adv.*, 2023, **13**, 19738

Efficient fluorescence-enhanced probe for cyanide ions based on a tetraphenylethene pyridine coordinated copper-iodide complex†

Fenqiang Luo,[a] Meng Guo,[a] Liyan Zheng *[c] and Zhixiong Cai *[b]

Received 1st May 2023
Accepted 26th June 2023

DOI: 10.1039/d3ra02868b

rsc.li/rsc-advances

An efficient fluorescence-enhanced probe was developed for detecting cyanide ions (CN^-) based on a tetraphenylethene coordinated copper-iodide complex (named CIT-Z). The coordination polymers (CPs) prepared were (*Z*)-1,2-diphenyl-1,2-bis[4-(pyridin-3-ylmethoxy)phenyl]ethene (**1Z**) and a CuI cluster, where the tetraphenylethylene (TPE) pyridine derivatives acted as organic ligands and the CuI cluster acted as a metal center. The higher-dimensional CIT-Z exhibited a 3-fold-interpenetrating network structure with excellent optical properties and chemical stability. This study also provides insights into the mechanism behind the fluorescence enhancement, which is attributed to the competitive coordination between CN^- and the ligands. The probe showed high selectivity and sensitivity towards CN^-, with a detection limit of 0.1 μM and good recovery in the real water samples.

Introduction

The cyanide ion (CN^-) is a toxic ion that has extremely strong toxicity to mammals and is very easily absorbed by the human body through oral, respiratory or skin contact.[1,2] It rapidly inactivates the oxygen transport function of cytochrome C oxidase by strongly binding to Fe^{3+} which is a hemin cofactor, thereby blocking cellular respiration.[3] CN^- is widespread in nature and can be produced and further metabolized by cyanogenic microorganisms or integrated and stored as cyanogenic glycosides in higher plants like sorghum, flax, giant taro, bamboo, and cassava.[2] The enzymatic release of cyanide from cyanogenic glycosides after cell rupture can lead to great danger and can cause severe chronic as well as significant acute public health problems.[3] Also, it is still widely used in many industrial activities, particularly in electroplating metallurgy and organic polymer production, which increases the risk of environmental contamination.[4,5] Therefore, a rapid and sensitive method for determination of CN^- is highly desirable in environmental monitoring, food safety, medical diagnosis and other fields.

Currently, various methods for detecting cyanide have been developed, including chromatography,[6] electrochemical,[7] or enzymatic techniques[8] and so on. However, several drawbacks are associated with traditional methods include high detection limits, complex operations, and lengthy detection time. As a result, fluorescent probe approaches have been extensively examined due to their convenience of use, quick detection, and low detection limits.[4,9–12] However, the stability of conventional organic small molecule fluorescent probes for cyanide detection, along with the utilization of toxic volatile organic solvents, imposes constraints on their wider application as practical sensors for cyanide.[13,14] Consequently, the pursuit of stable sensors based on organic and inorganic hybrid materials for the selective detection of CN^- ions in aqueous environments remains a challenging and crucial research area.

Coordination polymers (CPs) are a new type of intelligent material with a crystal framework that has received extensive attention.[15,16] They are mainly composed of organic ligands and metal ions or clusters. Therefore, charge transfer between the metal centers, ligands and between both can cause CPs to emit light.[17,18] CPs have important potential applications in chemical sensing, gas storage, compound separation, catalysis, optical devices and drug delivery.[19,20] Through the rational selection of metal centers, organic ligands or linkers, many CPs have inherent photoluminescence properties. For example, two-dimensional CPs that combine metal centers containing d^{10} electrons (Zn(II), Cd(II) or Cu(I)) with highly conjugated organic ligands typically exhibit ligand-dependent photoluminescence properties.[21] By modular synthesis of CPs with metal ions and organic ligands, various types of functional groups can be introduced into frameworks with unique properties. Recently, fluorescent probe molecules have been introduced to the pore

[a]*College of Chemical Engineering, College of Food and Biological Engineering, Collaborative Innovation Center of Fine Chemicals in Fujian Province, Zhangzhou Institute of Technology, Zhangzhou, 363000, China*

[b]*College of Chemistry, Chemical Engineering and Environment, Fujian Provincial Key Laboratory of Modern Analytical Science and Separation Technology, Minnan Normal University, Zhangzhou, 363000, China. E-mail: czx1816@mnnu.edu.cn*

[c]*School of Chemical Science and Technology, Yunnan University, Kunming, 650091, China. E-mail: zhengliyan@ynu.edu.cn*

† Electronic supplementary information (ESI) available. See DOI: https://doi.org/10.1039/d3ra02868b

surface of CPs as support or guest molecules.[22,23] CPs are highly ordered and tunable structures that have great application prospects in fabrication of chemical sensors.[24] The addition of guest molecules usually changes the optical properties of the main body of the coordination polymer, showing sensing applications for biological molecules, metal ions, explosives and environmental toxins.[25]

CPs have rich skeleton structures and adjustability, as well as rich topological structures, which have attracted much attention in the fields of fluorescence detection, catalysis, adsorption and drug delivery.[26,27] Among them, transition metal CPs have received more and more attention from researchers due to their diverse coordination modes.[28,29] Copper is widely available, has low raw material costs, is environmentally friendly and has low toxicity. It is more attractive from both economic and environmental perspectives. At the same time, copper(I) complexes have excellent optical properties, diverse coordination structures and good solution processability and have received extensive attention from researchers.[30] Although many copper(I) complexes with good optical properties and catalytic properties have been reported,[31] copper(I) ions are extremely unstable in aqueous solutions and air and are prone to disproportionation reactions. The coordination mode of copper complexes is relatively fixed. Developing new copper(I) complexes to improve their chemical stability, enrich their functions and expand their application fields is of great significance.

As a representative molecule in the field of aggregation-induced emission (AIE), tetraphenylethylene (TPE) has freely rotatable benzene rings, and different degrees of conformational distortion may lead to changes in optical properties.[32,33] TPE pyridine derivatives as organic ligands can obtain higher-dimensional CPs with excellent optical properties and novel structures. It is of great significance to design and develop more new TPE derivatives and expand their applications.

Herein, a CPs (named CIT-Z) was prepared using TPE pyridine derivative as an organic ligand and copper iodide as a metal center according to our previous work.[34] The CPs exhibits a two-dimensional triple-interpenetrating network structure with excellent chemical stability and optical properties. Based on its structural characteristics and the interaction between it and target analytes, CIT-Z can be utilized for detecting various pollutants in the environment. Due to its superior thermal and chemical stability, it can be employed for CN^- detection in aqueous solution. By utilizing competitive coordination between CN^- and ligands, CIT-Z fluorescence is enhanced with good selectivity and sensitivity.

Experimental section

Materials and methods

See the ESI.†

Synthesis of ligand TPE-2by-2-Z

The ligand TPE-2by-2-Z was synthesized according to the synthetic method in previous work.[35,36] The synthesis route is shown in Fig. 1. TPE-2OH (750 mg, 2.5 mmol) and 3-(bromomethyl)pyridinium hydrobromide (750 mg, 2.5 mmol) were fully mixed with potassium *tert*-butanolate (840 mg, 7.5 mmol) in 50 mL of toluene, refluxed at 110 °C under nitrogen protection for 12 hours. After neutralization and rotary evaporation to remove the solvent, the concentrated product was extracted with water and dichloromethane, and the extracted product was dried with anhydrous sodium sulfate. Rotary evaporation was used to remove dichloromethane, and the crude product was purified by column chromatography (ethyl acetate : petroleum ether = 1 : 3) to obtain two white solids TPE-2by-2-Z (yield, 30%) and TPE-2by-2-E (yield, 34%). See the details in Fig. S1–S3.†

TPE-2by-2-Z: ^{1}H NMR (400 MHz, $CDCl_3$, 25 °C) δ (TMS, ppm) 8.67 (2H, s) 8.59 (2H, s) 7.79 (2H, d, J = 8 Hz) 7.33–7.36 (2H, m) 7.07–7.10 (6H, m) 7.02 (4H, d, J = 4 Hz) 6.97 (4H, d, J = 8 Hz) 6.74 (4H, d, J = 8 Hz) 5.03 (4H, s). ^{13}C NMR ($CDCl_3$) δ (TMS, ppm) 156.82, 149.32, 148.93, 143.96, 139.75, 137.09, 135.39, 132.63, 132.57, 131.36, 127.74, 127.62, 126.31, 123.51, 114.62, 113.91, 67.42. HRMS: m/z calculated for $C_{38}H_{31}N_2O_2$ $[M + H]^+$ 547.238, found 547.238 (high resolution).

Synthesis of the CPs CIT-Z

The CPs CIT-Z was synthesized by dissolving TPE-2by-2-Z ligand (55 mg, 0.1 mmol) and cuprous iodide (19 mg, 0.1 mmol) in 4 mL of *N*,*N*-dimethylformamide (DMF) and 2 mL of acetonitrile, and then placing it in a 25 mL round-bottom flask. After stirring at room temperature for 4 hours, the mixture was centrifuged. The product after centrifugation was washed three times with DMF, acetonitrile, and methanol in turn, and then dried at 40 °C under vacuum for 10 hours to obtain pure CIT-Z. The yield was determined to be 82% based on copper. At room temperature, CIT-Z crystals were prepared by solvent diffusion method. Specifically, 6 mg of ligand was dissolved in 2 mL of DMF, followed by the slow addition of a mixed solution of 2 mL of DMF and acetonitrile (1 : 1), and finally the slow addition of a solution of 2 mg mL^{-1} cuprous iodide in acetonitrile. After three days, a single crystal was obtained in a stable state. Details of the crystal data are listed in Table S1.†

Results and discussion

Single crystal structure analysis of CIT-Z

Single crystal X-ray diffraction analysis was used to determine the crystal structure of coordination polymer CIT-Z. The crystal was found to crystallize in monoclinic space group $P2_1/n$ with a chemical formula of $[C_{38}H_{30}CuIN_2O_2]_n$. Cuprous iodide forms a four-coordinate Cu_2I_2 secondary building unit that coordinates with N atoms from four different ligands. Each adjacent Cu_2I_2 cluster is connected by ligands to form a two-dimensional network structure. More detailed structural analysis found that the rings in the same layer of the network are locked together to form a triple interpenetrating network structure of CIT-Z in the ab direction. The layers are connected by C–H$\cdots\pi$ interactions (Fig. S4†).[34] Powder X-ray diffraction pattern (PXRD) of the ligand and CIT-Z powder were compared with the simulated pattern generated by Mercury 4.1.0 software, and it was found

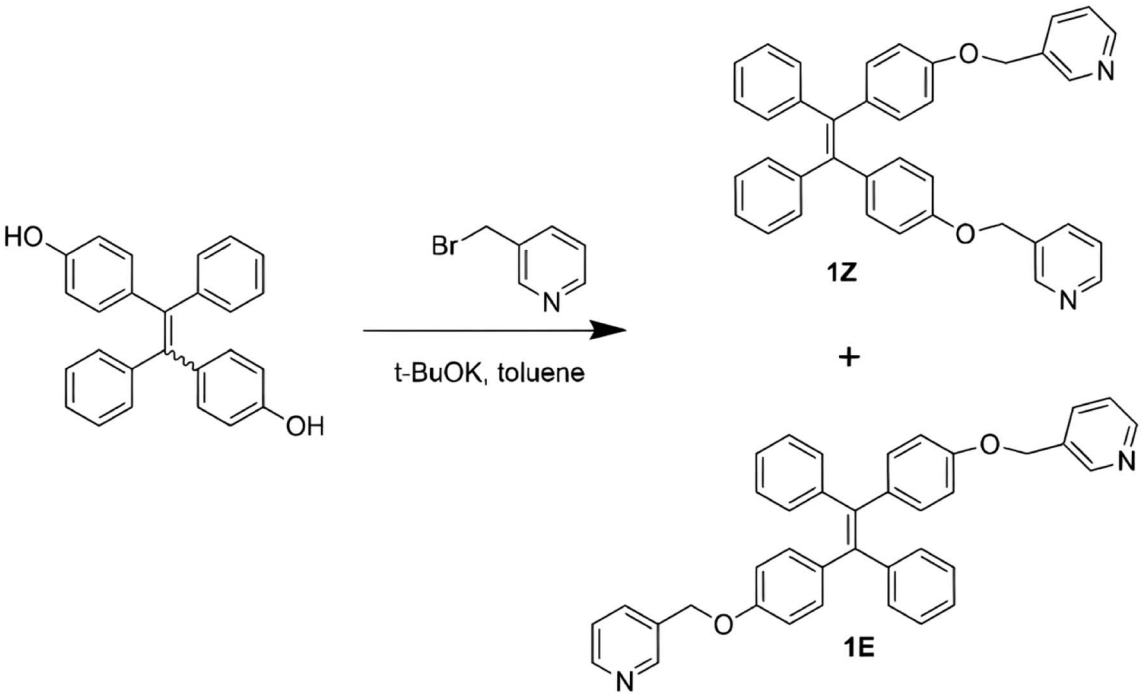

Fig. 1 Synthesis routes of 1Z and 1E.[36]

that the main diffraction peaks in the CIT-Z test pattern match well with the simulated pattern (Fig. 2). The crystal sample synthesized by the above method is highly pure.

Infrared (IR) and Raman spectroscopic analysis of CIT-Z

Infrared (IR) and Raman absorption spectroscopy tests were conducted on samples of the ligand and CIT-Z to analyze the skeletal and functional group information in their structures (Fig. S5†). Upon coordination of the ligand with cuprous iodide, the out-of-plane bending vibration of pyridine at 773 cm^{-1}, the stretching vibration of pyridine C=N at 1508 cm^{-1}, and the infrared characteristic absorption peak of TPE ring at 1575 cm^{-1} were all weakened. The Raman spectrum showed that the ring breathing signal of pyridine in CIT-Z was significantly enhanced after coordination. These results indicate that the ligand TPE-2by-2-Z successfully coordinated with cuprous iodide to synthesize coordination polymer CIT-Z.

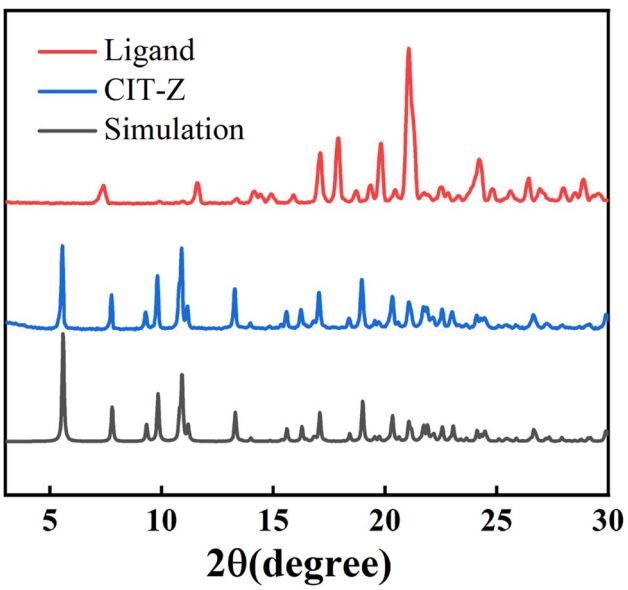

Fig. 2 PXRD patterns of ligand TPE-2by-2-Z and CIT-Z.

Stability study of CIT-Z

CIT-Z exhibits excellent thermal and chemical stability. A series of pH buffer solutions were prepared using Tris–HCl, and CIT-Z powder was soaked in these pH buffer solutions for 20 hours. After centrifugation and drying, PXRD measurements were performed. As shown in Fig. 3A, there was no significant change in the diffraction peaks of CIT-Z, indicating excellent chemical stability. To verify its thermal stability, CIT-Z powder was heated from 50 °C to 180 °C, and the PXRD spectrum showed no significant changes (Fig. 3B). At the same time, the thermogravimetric curve under nitrogen atmosphere also showed that CIT-Z did not exhibit weight loss until 350 °C, indicating excellent thermal stability (Fig. 3C). Excellent thermal and chemical stability are of great significance for the subsequent application of CIT-Z.

Study on the detection performance of CIT-Z for CN^- in water

TPE is a typical AIE molecule with a freely rotating benzene ring, and its optical properties are strongly dependent on its spatial conformation. This means that even small conformational differences can have a significant impact on its optical

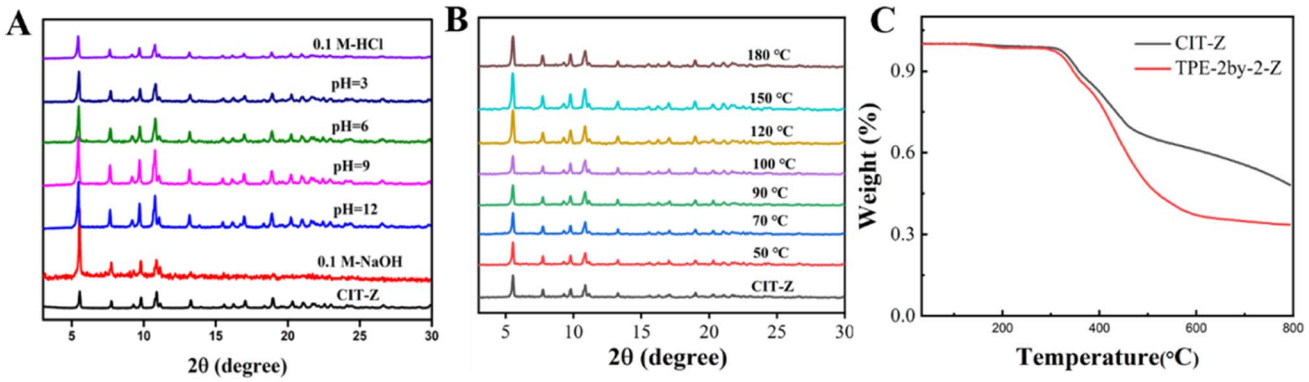

Fig. 3 PXRD pattern of CIT-Z at (A) different pH and (B) different temperatures; (C) thermogravimetric curves of ligand and CIT-Z.

properties. Cuprous complexes have excellent photophysical properties, diverse coordination structures, unique luminescent properties, and good processability.

Detection performance of CIT-Z for CN^-

CIT-Z has a triple network interpenetrating structure and good stability in aqueous solution, which enables its exploration of ion detection in aqueous solutions. To prepare the probe, a suspension of CIT-Z at a concentration of 1 mg mL^{-1} was formulated. Fig. 4A illustrates the emission and excitation spectrum of CIT-Z, providing insights into its fluorescence properties. The fluorescence lifetime of CIT-Z is measured to be 0.44 ns, indicating the average duration of its excited state before returning to the ground state. Additionally, the quantum yield of CIT-Z is determined to be 2.65%, representing the efficiency of CIT-Z in converting absorbed photons into emitted fluorescence. Due to the significant difference in luminescence performance between CIT-Z and ligands, it is considered to detect ligands with strong sub-copper coordination ability through competitive coordination. The detection of CIT-Z for CN^- in aqueous solution has selective response, and its fluorescence intensity increased by 1 fold (Fig. 4B). The fluorescence performance of CIT-Z upon various ions (CN^-, CO_3^{2-}, SO_4^{2-}, Ni^{2+}, NO_3^-, HCO_3^-, HPO_4^{2-}, Cl^-, Na^+, K^+, Zn^{2+}, HPO_4^-) were investigated, and it was found that it had specific response to CN^-. CIT-Z powder was ultrasonically dispersed in ultrapure water, and a suspension with a concentration of 1 mg mL^{-1} was mixed with 0.2 mM CN^-, 2 mM CO_3^{2-}, SO_4^{2-}, Ni^{2+}, NO_3^-, HCO_3^-, HPO_4^{2-}, Cl^-, Na^+, K^+, Zn^{2+} and HPO_4^- aqueous solutions, respectively. The emission spectra were measured after 20 min as shown in Fig. 4C.

The detection conditions of CIT-Z for detecting CN^- in aqueous solution were investigated. CN^- was added to the CIT-Z dispersed aqueous solution to determine the response time (Fig. 5C). The fluorescence of the solution was observed to increase significantly after approximately 1 min and was subsequently measured every 5 min thereafter. The fluorescence intensity of the solution remained stable after 20 min, indicating that its response time is both fast and stable. To determine the linear range of CIT-Z for detecting CN^-, the effect of different concentrations of CN^- on the fluorescence intensity of the solution was explored. Therefore, a CIT-Z dispersed aqueous solution with a CN^- concentration of 1–500 μM was prepared, and its emission spectrum was measured. As shown in Fig. 5A and B, with the increase of CN^- concentration, the luminescence intensity of CIT-Z gradually increased. In the range of 1–500 μM, its fluorescence intensity is linearly proportional to CN^- concentration, and the linear equation is $I = 0.61C + 460$ with a straight line fitting degree $R^2 = 0.998$. Therefore, CIT-Z can realize quantitative detection of cyanide

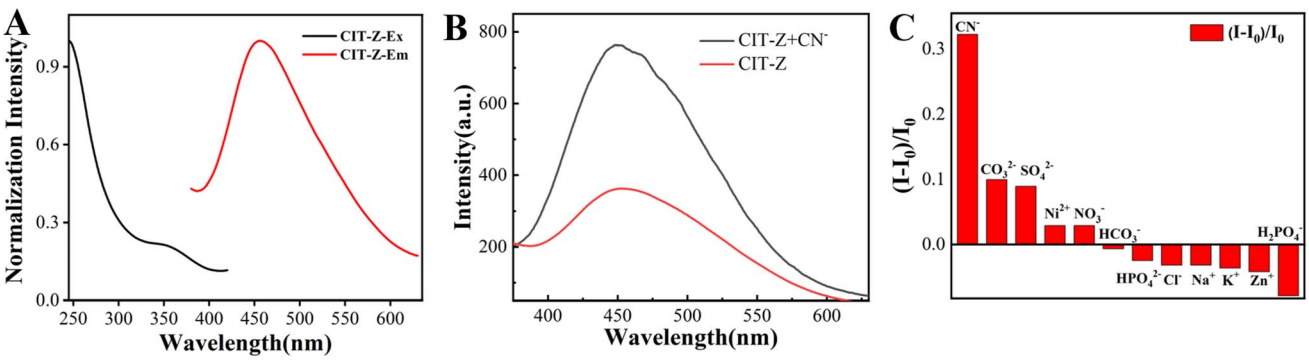

Fig. 4 (A) Emission and excitation spectrum of CIT-Z, (B) emission spectrum of CIT-Z before and after adding of CN^-, (C) CIT-Z response selectivity to a variety of ion.

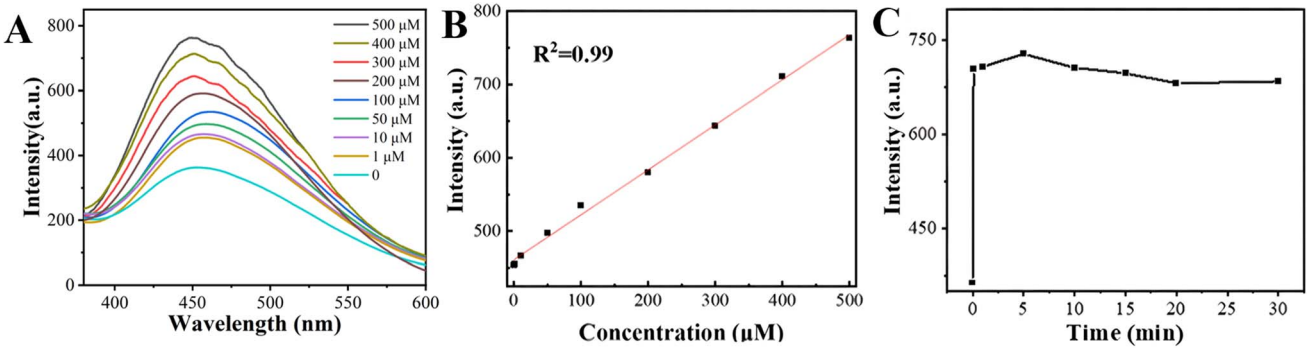

Fig. 5 (A) Emission spectra of CIT-Z in aqueous solutions of CN^- at different concentrations, (B) linear fitting plot and (C) plot of CIT-Z used to detect CN^- response time.

ions in the concentration range of 1–500 μM, and the detection limit of the sensor was calculated to be 0.1 μM (S/N = 3).

In the process of detecting water samples, there are often multiple coexisting interfering ions. Therefore, the effect of CIT-Z on CN^- detection under the coexistence of interfering ions was further investigated. A series of CIT-Z dispersed aqueous solutions coexisting with interfering ions and CN^- were prepared, where the concentration of interfering ions was 1.0 mM, the concentration of CN^- was 0.1 mM, and the concentration of CIT-Z was 0.5 mg mL^{-1} (Fig. 6). Under the conditions where interfering ions exist, CIT-Z can still quantitatively detect CN^-.

To verify the practicality of CIT-Z detection, actual water samples were taken to detect CN^- concentration after adding CN^- standard solution. Three replicate lake water samples were subjected to spiking with an unknown amount of CN^- standard solution to simulate samples. The obtained results, was labeled as "Found a", presented in Table 1, revealed CN^- concentrations of 0.1311 μM, 0.1008 μM and 0.1443 μM of in lake water. Subsequently, the samples were further spiked with an equal amount of standard solution to generate "Found b". The recovery rate was then calculated based on the measured concentrations of the target analyte. As depicted in Table 1, the recovery rate for CIT-Z detection ranged from 92.3% to 106.0%, highlighting the strong feasibility of CIT-Z for accurate detection of CN^- in actual samples. These findings demonstrated the suitability of the probe for accurate detection of CN^- in real-world water samples.

To comprehensively evaluate the advantages of the developed sensor, we conducted a performance comparison between the CN^- fluorescence sensor utilizing CIT-Z and other sensing functional materials, as summarized in Table S1.† The results of this comparison reveal several noteworthy findings. Firstly, the present CN^- fluorescence sensor based on CIT-Z exhibits an exceptional linear response range spanning three orders of magnitude, which surpasses the performance of many existing CN^- sensors. Furthermore, the detection limit achieved by the developed CN^- fluorescence sensor is comparable to that of recently reported CN^- sensors, highlighting its sensitivity. Notably, the limit of detection (LOD) for CN^- using CIT-Z (0.1 μM) is significantly lower than the drinking water guidelines set by the World Health Organization (1.9 μM), emphasizing its suitability for detecting low concentrations of CN^- in water samples.

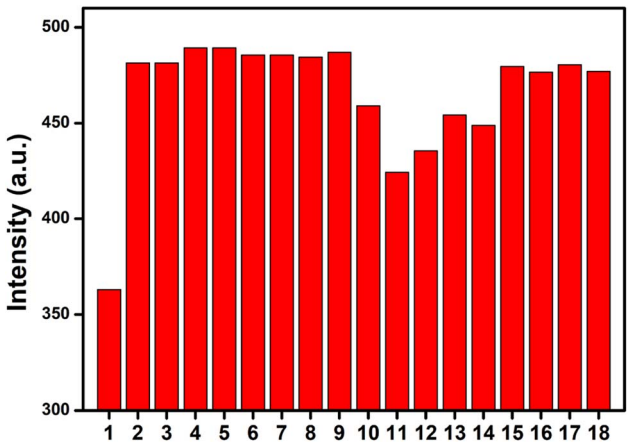

Fig. 6 Anti-interference experiment of CIT-Z for detecting CN^- ((1) blank; (2) CN^-; (3) Na^+; (4) K^+; (5) SO_4^{2-}; (6)CH_3COO^-; (7) Zn^{2+}; (8) HPO_4^{2-}; (9)HCO_3^-; (10) $H_2PO_4^{2-}$; (11) CO_3^{2-}; (12) Cl^-; (13) Fe^{3+}; (14) Fe^{2+}; (15) Co^{2+}; (16) Hg^{2+}; (17) Ni^+; (18) Mg^{2+}).

Mechanism of CIT-Z for CN^- detection

In general, the change in luminescence intensity of coordination polymers can be caused by three pathways: the analyte causes the collapse of the coordination polymer structure and releases the ligand, the analyte interacts with metal ions, and the analyte interacts with ligands.[37] Firstly, powder XRD tests were performed on CIT-Z treated with CN^-, as shown in Fig. 7A. The main diffraction peak position of CIT-Z did not change

Table 1 Analysis results of CN^- in water samples

Sample	Found a (mM)	Added (mM)	Found b (mM)	Recovery (%)
1	0.1311	0.01	0.1403	92.30%
2	0.1008	0.01	0.1106	98.36%
3	0.1443	0.01	0.1554	106.00%

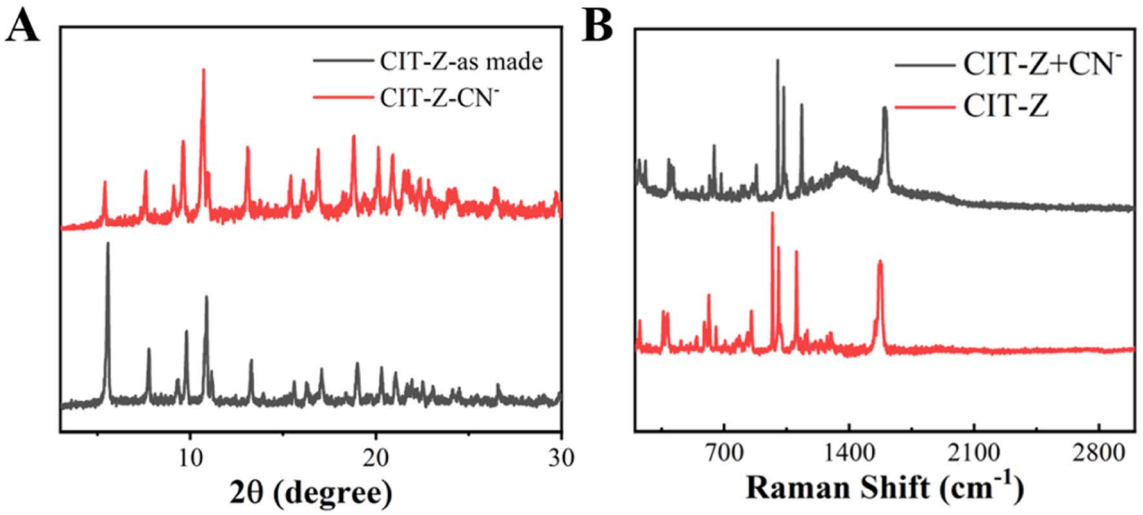

Fig. 7 (A) PXRD spectra of CIT-Z before and after cyanogen root treatment, and (B) Raman spectra of CIT-Z before and after cyanogen root treatment.

significantly before and after CN^- treatment, which excludes the possibility of collapse of coordination polymer framework. After CN^- treatment, SEM the morphology of CIT-Z did not change, which verified the XRD result (Fig. S6A and B†). Only the larger blocks exhibit a distinct transformation, resulting in the formation of smaller fragments. However, TEM images showed that small parts of complex edges were destroyed in CIT-Z after CN^- treatment (Fig. S6C and D†), which excluded the possibility of structural collapse and was most likely due to competition coordination between CN^- and ligands outside the interpenetrating network of CIT-Z that destroyed some Cu–N coordination bonds without destroying the network structure of CIT-Z.

To further verify the above hypothesis, IR and Raman tests were performed on CIT-Z treated with cyanide ions. As shown in Fig. 7B, after CN^- treatment, the Raman signal of C–N in-plane bending vibration at 1031 cm^{-1} was enhanced, and the IR characteristic absorption peak of TPE ring at 1575 cm^{-1} was enhanced (Fig. 8), which further verified the above conclusion. At the same time, as shown in Fig. S7,† the thermogravimetric results and fluorescence lifetime results of CIT-Z interpenetrated with CN^- were closer to those of the original CIT-Z. CN^- and ligands outside the interpenetrating network of CIT-Z competed for coordination without destroying the network structure of CIT-Z and without releasing ligands, which destroyed some Cu–N coordination bonds.

XPS test results showed that CIT-Z contains five elements: Cu, I, C, N and O, which is consistent with its structural analysis results (Fig. 9A). By fitting the C 1s peak, there was no significant alteration observed in the peak corresponding to C 1s (Fig. 9B). However, by fitting Cu 2p (Fig. 9C), the result showed that the Cu $2p_{1/2}$ (952.0 eV) and Cu $2p_{2/3}$ (932.1 eV) of the

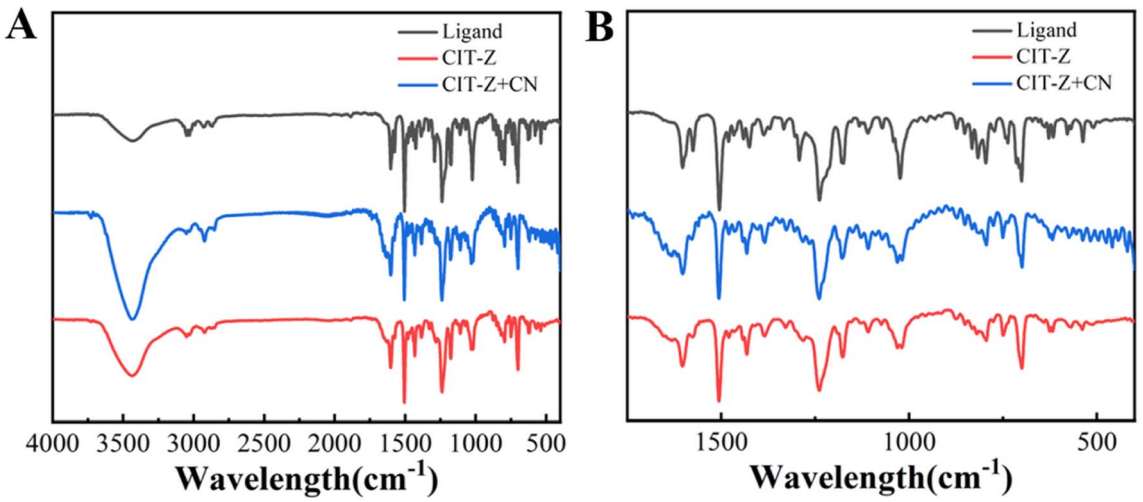

Fig. 8 IR spectra of CIT-Z and ligand before (A) and after (B) CN^- treatment.

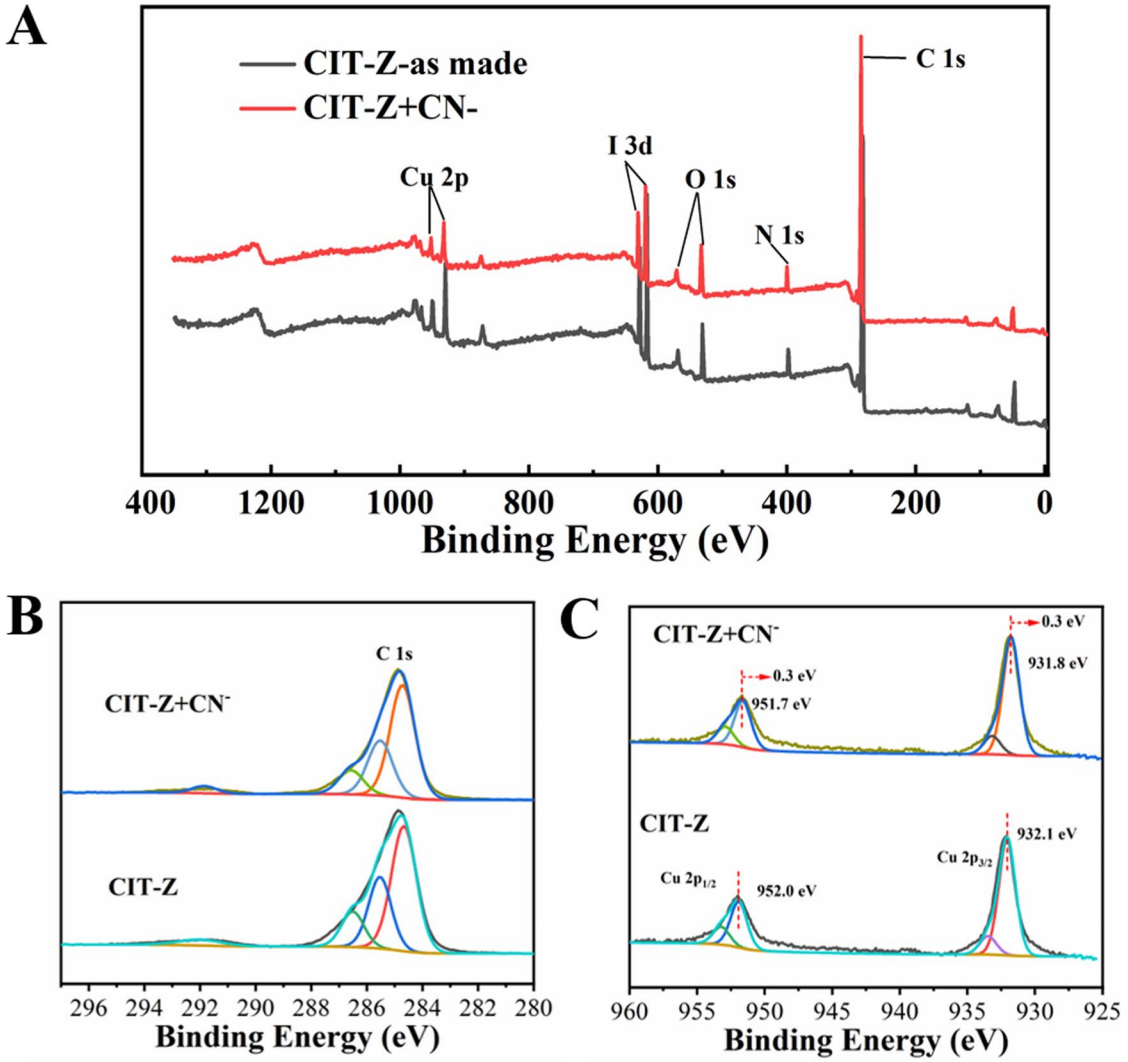

Fig. 9 (A) XPS full spectrum; fitting diagram of C 1s (B) and Cu 2p (C) photoelectron spectra of CIT-Z before and after CN^- treatment.

coordination polymer after CN^- treatment moves 0.3 eV towards lower binding energy direction, and the coordination environment of Cu changed, indicating that CN^- indeed participated in coordination. Therefore, the detection mechanism of CIT-Z for CN^- was as follows: CN^- competes with ligands outside the interpenetrating network of CIT-Z for coordination without destroying the network structure of CIT-Z and without releasing ligands, which destroyed a small part of Cu–N coordination bonds outside the network and enhanced its fluorescence.

Conclusion

A novel CPs CIT-Z with excellent optical properties was synthesized by solvent diffusion method and applied to the detection of CN^- in aqueous solution. The results showed that the two-dimensional coordination polymer CIT-Z was composed of ligand TPE-2by-2-Z and Cu_2I_2 clusters, which together constructed a two-dimensional triple-interpenetrating network structure of coordination polymer CIT-Z with excellent thermal stability and chemical stability. By using the competitive coordination between CN^- and ligands, CIT-Z fluorescence can be enhanced and applied to the detection of CN^- in aqueous solution with good selectivity and anti-interference ability. The detection linear range is 1–500 μM, and the detection limit is 0.1 μM, which is far lower than the industrial wastewater discharge standard.

Conflicts of interest

There are no conflicts to declare.

Acknowledgements

This work was supported by Doctoral Research Initiation Fund of Zhangzhou Institute of Technology (ZZYB2208), Education and Research Project for Middle and Young Teachers in Fujian Province (JAT220691), the National Natural Science Foundation of China (Grant No. 21964020 and 21904055) and the Nature Science Foundation of Fujian Province (Grant No. 2020J05164).

References

1 A. H. Hall, G. E. Isom and G. A. Rockwood, *Toxicology of Cyanides and Cyanogens: Experimental, Applied and Clinical Aspects*, John Wiley & Sons, 2015.
2 H. B. Leavesley, L. Li, K. Prabhakaran, J. L. Borowitz and G. E. Isom, *Toxicol. Sci.*, 2008, **101**, 101–111.
3 J. Parker-Cote, J. Rizer, J. Vakkalanka, S. Rege and C. Holstege, *Clin. Toxicol.*, 2018, **56**, 609–617.
4 F. Wang, L. Wang, X. Chen and J. Yoon, *Chem. Soc. Rev.*, 2014, **43**, 4312–4324.
5 K. Kulig, *Medical Aspects of Chemical and Biological Warfare*, ed. F. Sidell, E. T. Takafuji and D. R. Franz, TMM Publication, Washington, DC, 1997, pp. 271–286.
6 B. Desharnais, G. Huppé, M. Lamarche, P. Mireault and C. D. Skinner, *Forensic Sci. Int.*, 2012, **222**, 346–351.
7 S. Dadfarnia, A. M. Haji Shabani, F. Tamadon and M. Rezaei, *Microchim. Acta*, 2007, **158**, 159–163.
8 N. Wan, Z. Liu, F. Xue and Y. Zheng, *J. Biotechnol.*, 2015, **214**, 27–32.
9 L. Shang, L. Jin and S. Dong, *Chem. Commun.*, 2009, 3077–3079.
10 L. Long, M. Huang, N. Wang, Y. Wu, K. Wang, A. Gong, Z. Zhang and J. L. Sessler, *J. Am. Chem. Soc.*, 2018, **140**, 1870–1875.
11 W. Zhang, Y. Luo, P.-h. Zhu, X.-l. Ni, C. Redshaw, Z. Tao and X. Xiao, *ACS Appl. Mater. Interfaces*, 2022, **14**, 37068–37075.
12 M. C. Ríos, N. F. Bravo, C. C. Sánchez and J. Portilla, *RSC Adv.*, 2021, **11**, 34206–34234.
13 R. Ali, S. K. Dwivedi, H. Mishra and A. Misra, *Dyes Pigm.*, 2020, **175**, 108163.
14 F. Wang, L. Gao, Q. Zhao, Y. Zhang, W. Dong and Y. Ding, *Spectrochim. Acta, Part A*, 2018, **190**, 111–115.
15 B. M. Trost and S. R. Angle, *J. Am. Chem. Soc.*, 1985, **107**, 6123–6124.
16 G. M. Whitesides, J. P. Mathias and C. T. Seto, *Science*, 1991, **254**, 1312–1319.
17 M. D. Allendorf, C. A. Bauer, R. Bhakta and R. Houk, *Chem. Soc. Rev.*, 2009, **38**, 1330–1352.
18 S. S. Nagarkar, S. Horike, T. Itakura, B. Le Ouay, A. Demessence, M. Tsujimoto and S. Kitagawa, *Angew. Chem.*, 2017, **129**, 5058–5063.
19 X. Zhang, W. Wang, Z. Hu, G. Wang and K. Uvdal, *Coord. Chem. Rev.*, 2015, **284**, 206–235.
20 P. Kumar, A. Deep, K.-H. Kim and R. J. Brown, *Prog. Polym. Sci.*, 2015, **45**, 102–118.
21 B. Joarder, A. K. Chaudhari and S. K. Ghosh, *Inorg. Chem.*, 2012, **51**, 4644–4649.
22 Y. Wang, Y. Xu, Z. Yang, X. Zhang, Y. Hu and R. Yang, *J. Colloid Interface Sci.*, 2021, **598**, 474–482.
23 A. Karmakar, P. Samanta, A. V. Desai and S. K. Ghosh, *Acc. Chem. Res.*, 2017, **50**, 2457–2469.
24 W. P. Lustig, S. Mukherjee, N. D. Rudd, A. V. Desai, J. Li and S. K. Ghosh, *Chem. Soc. Rev.*, 2017, **46**, 3242–3285.
25 M. Chen, L. Chen, H. Li, L. Brammer and J. Lang, *Inorg. Chem. Front.*, 2016, **3**, 1297–1305.
26 X. Y. Xu, X. Lian, J. N. Hao, C. Zhang and B. Yan, *Adv. Mater.*, 2017, **29**, 1702298.
27 G. Chakraborty, I. H. Park, R. Medishetty and J. J. Vittal, *Chem. Rev.*, 2021, **121**, 3751–3891.
28 N. Kumar, T. Rom, V. Singh and A. K. Paul, *Cryst. Growth Des.*, 2020, **20**, 5277–5288.
29 V. M. Santhini, C. Wäckerlin, A. Cahlík, M. Ondráček, S. Pascal, A. Matěj, O. Stetsovych, P. Mutombo, P. Lazar and O. Siri, *Angew. Chem., Int. Ed.*, 2021, **60**, 439–445.
30 J. Troyano, F. Zamora and S. Delgado, *Chem. Soc. Rev.*, 2021, **50**, 4606–4628.
31 Y. Liu, S. Yiu, C. Ho and W.-Y. Wong, *Coord. Chem. Rev.*, 2018, **375**, 514–557.
32 Y. Chen, *Mater. Today Chem.*, 2022, **25**, 100975.
33 J. Yu, L. Sun, C. Wang, Y. Li and Y. Han, *Chem.–Eur. J.*, 2021, **27**, 1556–1575.
34 Q. Wang, H. Fan, Q. Zhou, X. Chen, L. Wang, Z. Lu, S. Yang, L. Zheng and Q. Cao, *Inorg. Chem.*, 2021, **60**, 18870–18878.
35 O. V. Dolomanov, L. J. Bourhis, R. J. Gildea, J. A. K. Howard and H. Puschmann, *J. Appl. Crystallogr.*, 2009, **42**, 339–341.
36 Z. Lu, S. Yang, X. Liu, Y. Qin, S. Lu, Y. Liu, R. Zhao, L. Zheng and H. Zhang, *J. Mater. Chem. C*, 2019, **7**, 4155–4163.
37 S. Wu, Y. Lin, J. Liu, W. Shi, G. Yang and P. Cheng, *Adv. Funct. Mater.*, 2018, **28**, 1707169.